УДК 615.47

IGOR H. CHYZH, GRYGORIJ S. TYMCHYK, ROMAN O. GUBIYCHUK, OLEKSANDR V. KARAS

ZOOM VARIO-OPTICAL SYSTEMS OF OPTOELECTRONIC SENSORS WITH IMMOBILE COMPONENTS

National Technical University of Ukraine "Igor Sikorsky Kyiv Polytechnic Institute, 03056 Kyiv, Ukraine; e-mail: deanpb@kpi.ua
Vinnytsia National Technical University, Ukraine

Abstract: The main focus of this paper is on the application of adaptive optics elements in vario-optical systems of optoelectronic sensors. The aim is to provide vario-systems with variable values of their external paraxial parameters and characteristics under the condition of immobility of the system components. The basics of preliminary design of optical autofocusing systems, zoom-afocal systems and zoom-relay systems have been developed, which allow to synthesize such systems taking into account the requirements to their external characteristics and parameters. The results of studies of two-component vario-systems of these types with the use of liquid vario-lenses functioning on the effect of electro-wetting or on the use of elastomeric membrane, the shape of which is regulated by external mechanical pressure, are presented. These are the products of Corning® Varioptic®,. Optotune®. Studies of auto-focusing systems, Galileo- and Kepler-type zoom-afocal systems, and zoom-relay optical systems have shown the influence on their external paraxial parameters and on the size of their field of view of the working ranges of the optical power of vario-lenses and the diameters of their apertures. It is shown that it is possible to create zoom-optical systems of all the above-mentioned types using only two liquid vario-lenses. The influence of functional parameters of these liquid vario-lenses on the dimensions of optical systems is also shown. The materials of the article are addressed to specialists who create zoom-optical systems of optoelectronic sensors.
Keywords: liquid vario-lens, zoom-afocal system, zoom-relay system, auto-focus lens, zoom systems with immobile components
Анотація: Основна увага в цій статті приділяється застосуванню елементів адаптивної оптики у варіооптичних системах оптоелектронних сенсорів. Метою є забезпечення варіосистем змінними значеннями їх зовнішніх параксіальних параметрів та характеристик за умови нерухомості компонентів системи. Розроблено основи попереднього проектування оптичних систем автофокусування, зум-афокальних та зум-релейних систем, які дозволяють синтезувати такі системи з урахуванням вимог до їх зовнішніх характеристик та параметрів. Представлено результати досліджень двокомпонентних варіосистем цих типів з використанням рідинних варіолінз, що функціонують на ефекті електрозмочування або на використанні еластомерної мембрани, форма якої регулюється зовнішнім механічним тиском. Це продукти Corning® Varioptic®. Optotune®. Дослідження систем автофокусування, зум-афокальних систем типу Galileo та Kepler, а також оптичних систем з зум-релейним керуванням показали вплив робочих діапазонів оптичної сили варіолінз та діаметрів їх апертур на їх зовнішні параксіальні параметри та розмір їхнього поля зору. Показано, що можливо створювати зум-оптичні системи всіх вищезгаданих типів, використовуючи лише дві рідкі варіолінзи. Також показано вплив функціональних параметрів цих рідких варіолінз на розміри оптичних систем. Матеріали статті адресовані фахівцям, які створюють зум-оптичні системи оптоелектронних датчиків.
Ключові слова: рідка варіолінза, зум-афокальна система, система зум-релейного керування, об'єктив з автофокусуванням, системи зумування з нерухомими компонентами

DOI: 10.31649/1681-7893-2025-50-2-251-268

1. INTRODUCTION

The rapid development of microelectronics has led to the emergence of numerous sensors in which optical systems fulfil an important auxiliary and sometimes the main function.

Optics in sensors are used for transmission and formation of radiation streams that arrive to photoelectric analysers and carry information about the state of objects under observation.

This information is then used in automated process control systems, in measuring equipment, in systems of automated observation and control of the physical state of the surrounding space. Machine vision with functions of autofocusing on observation objects, optics of flying drones, sophisticated techniques of telescopies, microscopy, endoscopy, optical distance measurement, optical coherence tomography and many other technical means increasingly contain zoom optics, which significantly expands the functionality of these means.

In zoom-optical systems such as zoom lenses and pancratic lenses, which use optical components with fixed values of their optical forces, mechanical displacements of the components along the optical axis according to predetermined dependencies are required. The number of components in such systems is at least three or more and each of them has its own individual movement dependence. Most often these dependencies are essentially non-linear, which requires for their execution corresponding mechanisms that complicate the optical part of sensors, increase their size and cost. The need to eliminate this disadvantage has led to the development and appearance on the market of adaptive optical elements, which have the property to change the focal length within large limits under the action of external, more often electrical control. This provides conditions for the creation of zoom optics with fixed components, which significantly simplifies their design and eliminates the need for additional mechanisms for moving the components. At present, several principles of vario-lenses functioning are known [1].

Among them, liquid vario-lenses, operating on the basis of the electro-wetting effect, and liquid lenses in which two liquids with different refractive indices are separated by an elastomeric membrane, have been practically implemented. The shape of the membrane is controlled by over- or under-pressurisation of one of the fluid chambers [1].

These lenses are widely used in optical and optoelectronic devices [2- 24].

The currently known manufacturers of these lenses are Corning® Varioptic® and Optotune®, [25-26]. Corning® Varioptic® specialises in electrowetting vario-lenses. Optotune® specialises in elastomeric membrane variolenses. The main optical parameters of vario-lenses are the range of variation in optical power and the diameter of the window (light diameter) through which light passes in the lens. Lenses based on the electro-wetting effect have a relatively small light diameter but a relatively large range of optical power variation. They are also easy to control by applying electrical signals to the lens electrodes from a driver, providing optical power change times in milliseconds.

A-16F [+15 ÷ −5] dptr ∅1.6 mm | A-25H [+13 ÷ −5] dptr ∅2.5 mm | A-39N [+15 ÷ −5] dptr ∅3.9 mm | A-58N [+10 ÷ −5] dptr ∅5.8 mm

Their high degree of electronic integration is evidenced by the exterior view of the Corning® Varioptic® series of A-PE liquid lenses shown in the figure.

Below are liquid lenses from Optotune®, which have a significantly larger luminous diameter due to their membrane construction

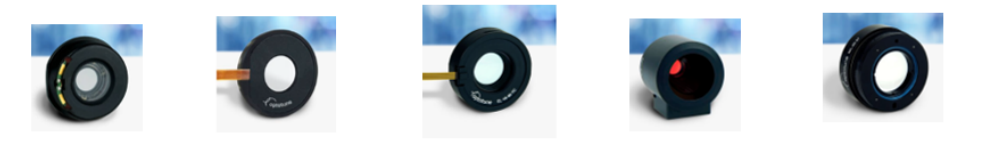

EL-3-10 [−13 ÷ +13] dptr ∅3 mm | EL-12-30 TC [−6 ÷ +10] dptr ∅12 mm | EL-16-40 TC [−10 ÷ +10] dptr ∅16 mm | EL-10-42 OF [−2 ÷ +2] dptr ∅8 mm | ML-20-37 [−18 ÷ +18] dptr ∅20 mm

Only one of the ML-20-37 lenses shown here is mechanically controlled by an external toothed ring, which can be rotated by a stepper rotor micromotor controlled by a microcontroller.

The above presented vario-lenses allow to synthesise practically all types of optical systems - lenses, zoom-afocal systems (telescopic with variable angular magnification), zoom-relay systems (projection systems with variable transverse magnification). The basic and fundamental requirement for such systems is mutual immobility of their optical elements.

A specific feature of liquid variolenses is that, as can be seen from the above, they have a limited range of variation of optical power and relatively small diameters of apertures free for the passage of light. This circumstance limits the main optical characteristics of systems assembled from such lenses - equivalent focal length, transverse or angular magnifications, the size of the field of view. In this connection, it seems reasonable to make a theoretical analysis of the functional capabilities of optical systems assembled on liquid vario-lenses and, on this basis, to propose working formulae for estimating the external functional parameters of such systems, which may be useful for developers of optoelectronic sensors.

2. MATERIALS AND METHODS

2.1 Vario lenses in the autofocus system

Figure 1 shows an optical system in which there is an objective lens with focal length fixed. In the following, such a lens will bewill be called a fixed lens.

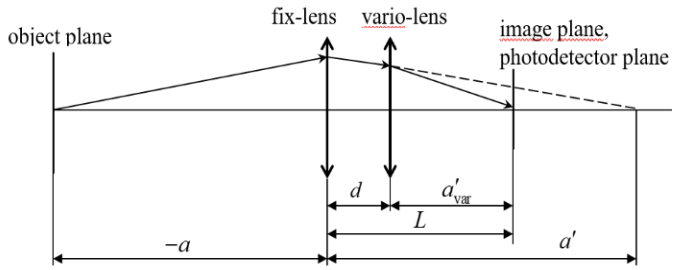

Figure 1 – Vario lenses in the autofocus system

There is an Object Plant (OP) in front of the fix-lens, the image of which must be accurately focused on the photodetector at any distance of the OP from the fix-lens.

If the distance from the fix-lens to the OP varies between infinity and the front focus of the lens, the image plane formed by the fix-lens moves from the photodetector plane to infinity.

With such a large range of movement of the OP, it is not possible to focus the image by changing the distance between the fix-lens and the photodetector.

The use of a pancratic lens instead of a fixed lens in this case, with its unchanged position relative to the photodetector, is a difficult task because of the need to keep its back focal length constant at large focal length changes.

The problem can be solved by installing a vario-lens behind the fixed lens, as shown in figure 1. A vario-lens can change its focal length under the control of external devices, which allows all elements of such an optical system to be stationary. An example of a vario-lens is the Optotune ML-20-37 lens [26], figure 2.

It is capable of changing its focal length between $-\infty$ до $-56\,\text{mm}$ and $+56\,\text{mm}$ до $+\infty$. At the same time, its optical power varies within ± 18 dioptres. The light diameter of this lens is 20 mm.

The optical power of the vario-lens is controlled by mechanically rotating its gear wheel using a miniature electric rotary stepper motor.

For this purpose, a gear with the same modulus as on the vario-lens is provided on the motor output shaft in contact with the gear with of the lens. In this case, the focal length adjustment of the vario-lens can be automated.

The mechanism for rotating the variolens gear with low torque to ensure reliable motorisation and repeatability of 0.1 dioptres. The dependence of the optical power or focal length of the vario-lens on the distance to the object whose image is to be focused on the photodetector is found under condition $L = F'_{fix}$.

Figure 2 – Vario-lens Optotune ML-20-37

Then at infinite distance to the plane of objects, the vario-lens must have zero optical power or, what is the same, infinite focal length $F'_{\text{var}} = \infty$.

According to the Gauss formula, when moving the subject plane to the fix-lens, the image moves away from it by the distance

$$a' = \frac{a \cdot F'_{fix}}{a + F'_{fix}}. \tag{1}$$

This primary image serves as the object for the vario-lens. The distance from this image to the vario-lens is $a_{\text{var}} = a' - d$

where d is the distance between the rear principal plane of the fix- lens and the front principal plane of the vario-lens.

In this case, the segment a'_{var} should provide the position of the secondary image formed by the vario-lens in the plane of the photodetector. Then the rear focal length of the vario-lens is determined by expression (2):

$$F'_{\text{var}}(a) = \frac{-a'_{\text{var}}\left[F'_{fix}(a-d) - ad\right]}{\left(F'_{fix}\right)^2}, \tag{2}$$

and the optical power of the variolens in diopters:

$$D_{\text{var}}[dptr] = \frac{-1000\left(F'_{fix}\right)^2}{a'_{\text{var}}\left[F'_{fix}(a-d) - ad\right]}. \tag{3}$$

Since the working range of the optical power of the vari-lens is limited, the desire to extend the working range of distance a , as can be seen from formulas (2) and (3), requires a decrease in distance d , which is accompanied by an increase in distance a'_F . Thus, under conditions $d = 0$ and $a'_{\text{var}} = F'_{fix}$, formula (3) takes the following form

$$D_{\text{var}}[dptr] = \frac{-1000}{a}$$

from which we can find the limit value of the segment

$$a_{\min}[\text{mm}] = -\frac{1000}{D^*_{\text{var}}[dptr]}, \tag{4}$$

where $a_{\min}[\text{mm}]$ is the minimum distance between the fix-lens and the subject plane $D^*_{\text{var}}[dptr]$, is the maximum possible value of the optical power of the vario-lens.

The Optotune ML-20-37 lens has $D^*_{\text{var}}[dptr] = 18$, while according to formula (4) $a_{\min}[\text{mm}] = -55.555\,\text{mm}$, and the entire working range of the distance from the lens to the OP $a \in [-\infty ... -55.555]\,\text{mm}$.

The minus sign indicates that the origin of the segment a is at the front main point of the fix- lens.

Figure 3 shows a graph illustrating the relationship between the distance value and the optical power of the Optotune ML-20-37 vario-lens.

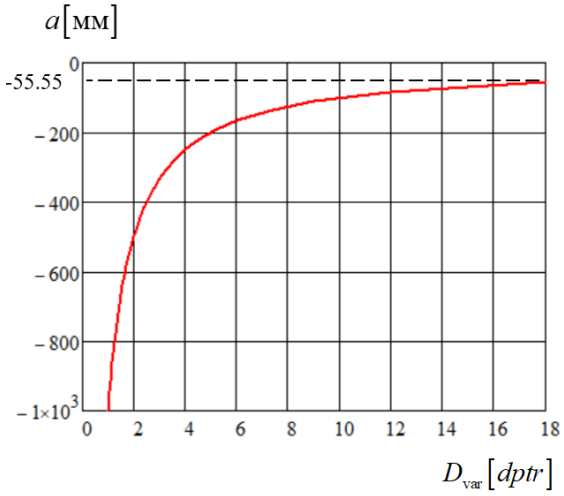

Figure 3 – Graph of dependence of the optical power of the vario-lens on the distance to the object

The graph in figure 3 is obtained under conditions: $F'_{fix} = 50\,\text{мм}$, $d = 0$ (the rear main principal point of the fix-lens is aligned with the front principal point of the vario-lens), $a'_F = 50\,\text{мм}$ (the distance between the rear principal point of the vario-lens and the photodetector plane

The value of $D_{\text{var}}[dptr]$ asymptotically approaches zero as the OP moves away from the fix- lens.

Linear magnification of the system shown in figure $\beta = \frac{y'}{y}$, , where is the size of the object in object plane , y' is the size of the image of the object in image plane.

If the field aperture of the optical system is the boundaries $(b \times c)$ of the photosensitive zone of the photodetector located in the image plane, then in this case the dimensions of the field of view in OP

$$B \times C = \frac{(b \times c)}{\beta}$$

Where

$$\beta = \frac{F'_{fix} \cdot F'_{\text{var}}}{(F'_{\text{var}} - d)(F'_{fix} + a) + F'_{fix} \cdot a}. \qquad (5)$$

Figure 4 shows a graph of the paraxial magnification versus the distance between the optical system and the OP.

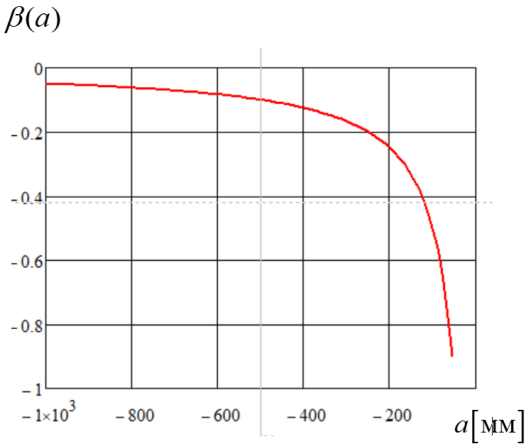

Figure 4 – Graph of the dependence of paraxial magnification on the distance between the optical system and the OP

The graph in figure 4 is obtained under the same conditions as the graph in figure 3. As can be seen, as the OP moves away from the optical system, the size of the field of view increases nonlinearly with respect to distance a . As distance a increases, the value of β asymptotically approaches zero.

If the OP contains an element whose linear dimensions Y are known a priori, then by estimating the dimensions of the image Y' after its autofocusing in the plane of the photodetector, it is possible to determine the value β as a ratio $\beta = \frac{Y'}{Y}$. Taking into account the focal length of the vario-lens F'_{var} at the moment of measuring the distance to OP, by formula (6) it is possible to determine the distance $a(\beta)$:

$$a(\beta) = \frac{F'_{fix} \cdot F'_{\text{var}} - \beta(F'_{\text{var}} - d)F'_{fix}}{\beta(F'_{fix} + F'_{\text{var}} - d)}. \tag{6}$$

It goes without saying that distortion, if present in the optical system, must be taken into account when determining the size Y' .

Thus, the optical autofocus system investigated here, equipped with a matrix photodetector and a system for controlling the optical power of the vario-lens, can serve as a sensor of distances to objects.

2.2 Zoom Afocal Systems

Zoom-afocal - telescopic systems with adjustable angular magnification. Such systems are used in laser beam expanders, transfocators, sensors, and other devices in which optical telescopic systems are used.

In zoom-afocal systems, where optical components with fixed optical forces are used, variable angular magnification is achieved by moving the components along the axis according to predetermined relationships. Such movements require special mechanisms. Here we consider the possibility and conditions for creating zoom-afocal systems with fixed components. As components of such systems it is supposed to use vari- lenses.

It is known that telescopic systems are of two types - the Galileo system and the Kepler system, [27]. Galileo systems, in which components have opposite signs of optical forces, create direct images. This is their essential advantage. The aperture diaphragm in them is the entrance pupil of the lens following the afocal system or the frame of the matrix photodetector [28,29].

The disadvantage of such systems is the absence of a real intermediate image OP, where the field aperture is installed, which provides a sharp limitation of the field of view. In these systems, the field of view is limited by the vignette aperture, due to which the field of view is not sharply limited. The angular size of the field of view of Galileo systems is considerably inferior to that of Kepler systems at the same angular magnification [30,31,32].

Kepler systems contain components with positive optical forces. For this reason, they form an inverted image. In these systems there is a valid intermediate image OP in which a field aperture can be set and thus a sharp limitation of the field of view can be achieved. In addition, the frame of one of the system components serves as an aperture diaphragm. This ensures that the entrance and exit pupil are independent of the existence of external components [33].

In connection with the above, it is reasonable to separately analyse the properties of zoom-afocal systems functioning according to the Galileo scheme and according to the Kepler scheme under the condition of immobility of their optical components.

2.2.1 *Galileo zoom-afocal system*

Figure 5 shows a Galileo telescopic system in which the first component has positive optical power ($D_{1\,\text{var}} > 0$) and the second component has negative optical power ($D_{2\,\text{var}} < 0$).

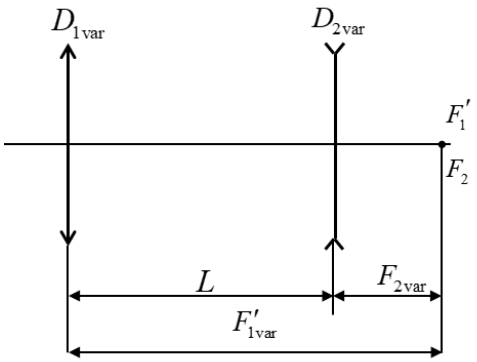

Figure 5 – Galileo optical system in thin variocomponents

The figure 5 shows that

$$L = F'_{1\,\mathrm{var}} - F_{2\,\mathrm{var}} = F'_{1\,\mathrm{var}} + F'_{2\,\mathrm{var}} = \frac{1}{D_{1\,\mathrm{var}}} + \frac{1}{D_{2\,\mathrm{var}}} \tag{5}$$

Angular magnification of the afocal system, [27]:

$$\gamma = -\frac{F'_{1\,\mathrm{var}}}{F'_{2\,\mathrm{var}}} = -\frac{D_{2\,\mathrm{var}}}{D_{1\,\mathrm{var}}} \tag{6}$$

The system composed of equations (5) and (6) has a solution with respect to the optical forces of the components :

$$D_{1\,\mathrm{var}} = \frac{\gamma - 1}{\gamma L}, \tag{7}$$

$$D_{2\,\mathrm{var}} = \frac{\gamma - 1}{L}. \tag{8}$$

In diopters, the optical powers of these components:

$$D_{1\,\mathrm{var}}[\mathrm{dptr}] = \frac{1000(\gamma - 1)}{\gamma L}, \qquad D_{2\,\mathrm{var}}[\mathrm{dptr}] = \frac{1000(1 - \gamma)}{L}.$$

Figure 6 shows graphs of dependences $D_{1\,\mathrm{var}}(\gamma)$ and $D_{2\,\mathrm{var}}(\gamma)$ obtained at different values of axial length L. If the Galileo zoom-focal system is composed of two identical Optotune ML-20-37 vario-lenses, which have an operating range of optical power of $\pm 18\,\mathrm{dptr}$, then the achievable values of angular magnification depend on the axial length of the system. Expansion of the angular magnification range, as can be seen from formulas (7), (8) and graphs in Fig.6, is possible by increasing the axial length of the system and extending the working range of the optical power of the vario-lenses.

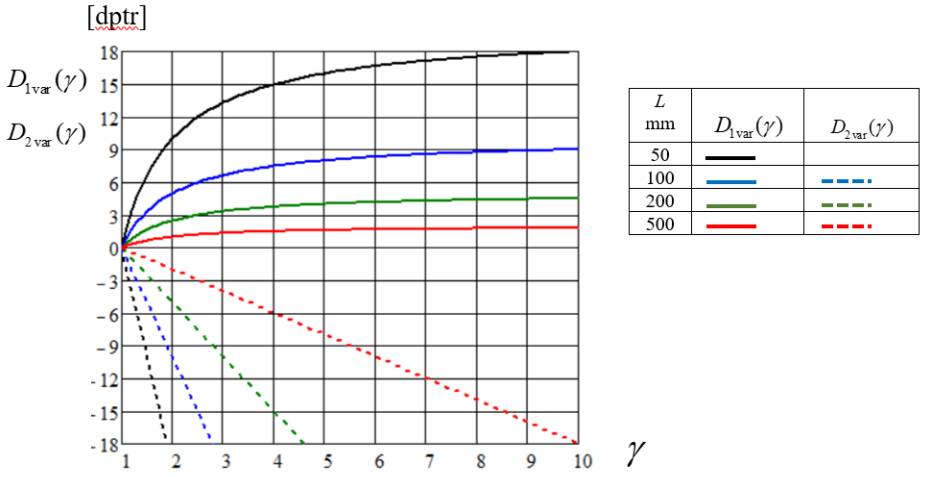

Figure 6 – Graphs of dependence of optical power of variocomponents on angular magnification of zoom-afocal system

The size of the field of view of Galileo systems is determined by the size of the vignetting aperture, which is usually the frame of the first component - the first variolens. If behind the Galileo system there is a fix-component, the frame of which serves as an (STOP) aperture, then the angular size of the field of view of the in the absence of vignetting in the visual field [27]:

$$2\omega[rad] = 2arctg\frac{\varnothing_1 - \gamma\varnothing_{STOP}}{2\gamma(\gamma t' + L)} \tag{9}$$

at full vignetting outside the field of view

$$2\omega[rad] = 2arctg\frac{\varnothing_1 + \gamma\varnothing_{STOP}}{2\gamma(\gamma t' + L)}\ , \tag{10}$$

where $\varnothing_1$ is the light diameter of the first component,

t' - removal of the STOP aperture from the second component of the Galileo system.

Formulas (9) and (10) show that at fixed values of diameters $\varnothing_1$ and $\varnothing_{STOP}$, an increase in the axial length of the system L and angular magnification γ is accompanied by a narrowing of the field of view.

2.2.*2 Kepler's zoom-afocal system*

Figure 7 shows Kepler's zoom-afocal system in thin components.

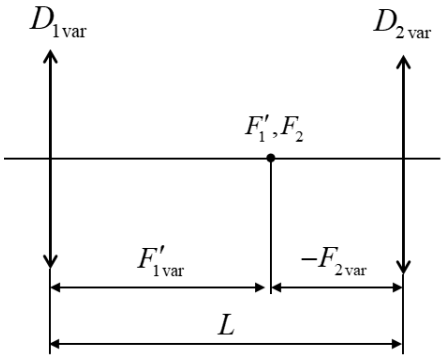

Figure 7 - Kepler's zoom-afocal system in thin components

According to this figure

$$F'_{1\,var} - F_{2\,var} = F'_{1\,var} + F'_{2\,var} = L\ , \tag{11}$$

$$\frac{f'_{1\,var}}{f'_{2\,var}} = -\gamma\cdot \tag{12}$$

From the system of equations (11), (12):

$$F'_{1\,var} = \frac{\gamma}{\gamma - 1}L\ , \tag{13}$$

$$F'_{2\,var} = \frac{1}{1-\gamma}L\cdot \tag{12}$$

Optical powers of variolenses in diopters:

$$D_{1\,var}(\gamma)[dptr] = \frac{1000(\gamma - 1)}{\gamma L}\ , \tag{15}$$

$$D_{2\,var}(\gamma)[dptr] = \frac{1000(1-\gamma)}{L}\cdot \tag{16}$$

In formulas (13) to (16), the angular magnification γ has a negative sign because the Kepler system forms an inverted image.

Figure 8 shows the graphs of functions $D_{1\,\mathrm{var}}(\gamma)[dptr]$ and $D_{2\,\mathrm{var}}(\gamma)[dptr]$, for example, adapted to the parameters of the Optotune ML-20-37 vario-lens, which has the largest range of variation of optical power and the largest luminous diameter.

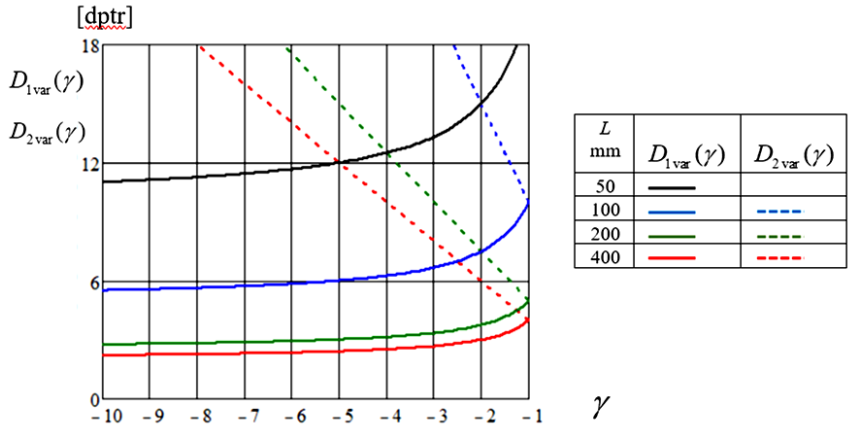

Figure 8 – Graphs of dependences of optical power of components on angular magnification

It follows from the above plots that the possible range of values of angular magnification is significantly limited both by the range of the optical power of the second vario-lens and by the axial length of the optical system. This is due to the fact that in the Kepler system, in contrast to the Galileo system, both components have a positive optical power. The range of angular magnification of the Kepler system is limited by the maximum value of the optical power of the second component.

For the Optotune ML-20-37 vario-lens, which has $D_{\max} = 18\,dptr$, even to obtain an angular magnification of $\gamma = -1$ according to formula (16) requires an axial length of the system of at least 111.11 mm. If the value L is given, the maximum possible magnification of the Kepler system can be determined from formula (16)

$$\gamma_{\lim} = 1 - \frac{L\left(D_{2\,\mathrm{var}}\right)_{\max}}{1000} \tag{17}$$

where $\left(D_{2\,\mathrm{var}}\right)_{\max}$ is the largest dioptre value of the optical power of the second vario-lens

Formula (17) indicates that at a fixed value of the maximum optical power of the second vario-lens the growth of the value $|\gamma_{\lim}|$ is possible only when the length of the system is increased L. The above also shows that at the same axial length of the Galileo and Kepler systems the latter has smaller limits of providing the required values γ.

In those cases when, due to dimensional limitations of axial length, the Kepler system composed of two variolenses does not provide the required range of values γ, the extension of this range of values can be achieved by installing an additional lens with a fixed value of optical power D_{fix} in the vicinity of the second variolens. Such a method may be rational for compensation of aberrations of the vario-lens. In this case, the total optical power of the double component [27]:

$$D_{\Sigma\,\mathrm{var}}(\gamma) = D_{fix} + D_{2\,\mathrm{var}}(\gamma) - d \cdot D_{fix} \cdot D_{2\,\mathrm{var}}(\gamma), \tag{18}$$

where d is the distance between the rear principal point of the fix-lens and the front principal point of the vario-lens. Since the front principal point of the variolens is always inside the lens, the special shape of the fix-lens allows its rear principal point to be moved outside the lens and aligned with the front principal point of the variolens, thus ensuring the condition $d = 0$. In this case

$$D_{\Sigma\,\mathrm{var}}(\gamma) = D_{fix} + D_{\mathrm{var}}(\gamma). \tag{19}$$

In this way, the range of variation in optical power of vario-lenses in other optical systems can be shifted as needed.

2.2.3 *Field of view of the zoom-afocal system according to Kepler's scheme*

In a conventional afocal system according to Kepler's scheme, the field of view is limited by a field aperture, which is located in the plane of the combined focal points $F_1'F_2$, Fig. 7. As the optical forces of the component optical forces vary, the points $F_1'F_2$ are displaced along the optical axis. This requires moving along the axis of the field diaphragm, possibly changing its diameter, which contradicts the initial condition of immobility in the system of all its components. It follows that the presence of a field diaphragm in a zoom-afocal system according to the Kepler scheme with stationary components is impossible. In this case, the field of view can be limited by a vignetting aperture.

If the zoom-focal system is composed of a vario-lens with a rear lens having a light diameter not less than the light diameter of the front lens, and the zoom-afocal system operates in mode $|\gamma| \geq 1$, then the front lens barrel serves as an aperture diaphragm and the rear lens barrel as a vignetting diaphragm. In this case, the size of the field of view is determined taking into account the value of the vignetting coefficient k .

Fig. 9 shows the angles $\omega_{k=1}$, $\omega_{k=0}$ of inclination of two beams of rays, at which one beam has no vignetting of rays $(k=1)$, Fig. 9 (a), and the second beam has full vignetting of rays $(k=0)$, Fig. 9 (b).

The condition of absence of vignetting of the beam of rays filling the light aperture of the front vario-lens is complete passage of this beam through the aperture of the rear vario-lens. The greatest inclination of the unvignetised beam of rays at the entrance to the system takes place when the ray with number 1, in Fig. 9 (a) passes through the lower edge of the rear lens aperture. In this case, the angle of the field of view in the space of objects in the absence of vignetting:

$$2\omega_{k=1} = 2arctg\left[0.5\left(\frac{\varnothing_1 + \varnothing_2}{L} - \frac{\varnothing_1}{F'_{1\text{var}}}\right)\right] \tag{20}$$

The condition of complete vignetting of the beam of rays filling the light aperture of the front vario-lens is complete non-passage of this beam through the aperture of the rear vario-lens. The greatest inclination of the fully vignetted ray beam at the entrance to the system occurs when the ray with number 3, in Fig. 9 b) passes through the lower edge of the rear lens aperture.

In this case, the angle of the field of view in the space of objects at full vignetting:

$$2\omega_{k=0} = 2arctg\left[0.5\left(\frac{\varnothing_2 - \varnothing_1}{L} + \frac{\varnothing_1}{F'_{1\text{var}}}\right)\right]. \tag{21}$$

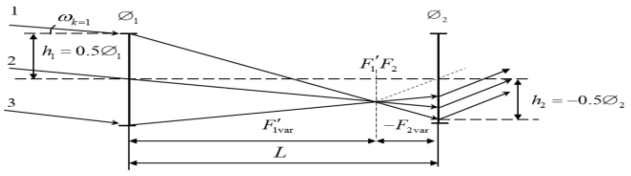

a)

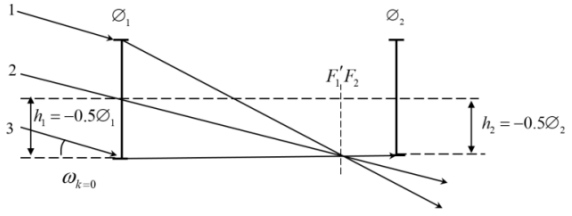

b)

Figure 9 – Passage of edge ray beams through the Kepler system:
(a) with no vignetting, (b) with full vignetting

According to expression (17) the length of the system

$$L = (1 - \gamma_{\lim})F'_{2\min},$$

where $\gamma_{\lim}$ is the limiting value of angular magnification,

$F'_{2\min}$ - limit minimum value of the back focal length of the second vario-lens.

Substituting this expression into (20), (21), we obtain the dependence of the angular size of the field of view of the system on the limiting value of angular magnification:

$$2\omega_{k=1} = 2arctg\left\{\frac{1}{2F'_{2\min}}\left[\frac{\varnothing_2\gamma_{\lim} + \varnothing_1}{(1-\gamma_{\lim})\gamma_{\lim}}\right]\right\}, \tag{22}$$

$$2\omega_{k=0} = 2arctg\left\{\frac{1}{2F'_{2\min}}\left[\frac{\varnothing_2\gamma_{\lim} - \varnothing_1}{(1-\gamma_{\lim})\gamma_{\lim}}\right]\right\}. \tag{23}$$

Figure 10 shows graphs of the dependence of the angular size of the field of view on the limiting value of the angular magnification of the Kepler system. For the example, the Optotune ML-20-37 vario-lens is again taken, which has a light diameter of 20 mm and a minimum focal length value of 55.(5)mm ($\varnothing_1 = \varnothing_2$ =20 mm, $F'_{2\min} = 55.(5)$ мм).

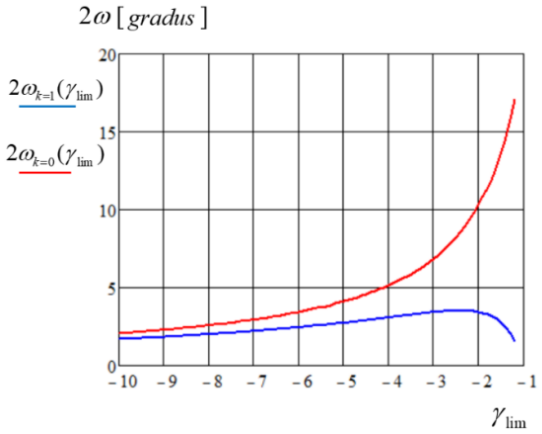

Figure 10 – Graphs of dependence of the size of the field of view of the Kepler system on the angular magnification at k=1 and at k=0

The graphs presented in Fig. 10 show that as the absolute value of angular magnification γ increases, the size of the field of view decreases, which is caused by the growth of the axial length of the system at constant light diameters of the variolenses. Moreover, the sizes of the field of view without vignetting of rays and with full vignetting of rays asymptotically converge.

2.3 *Zoom-relay lenses*

Figure 10 shows a zoom projection optical system in which the intervals a_1, d_1, a'_2 are fixed and unchanging. The transverse magnification β in the optically conjugate object (OBJ) and image (IMA) planes is intended to be variable over a specified range. Vario-lenses 1 and 2 are designed to vary their optical powers $D_{1\,\mathrm{var}}(\beta)$ and $D_{2\,\mathrm{var}}(\beta)$ to provide the desired magnification value β .

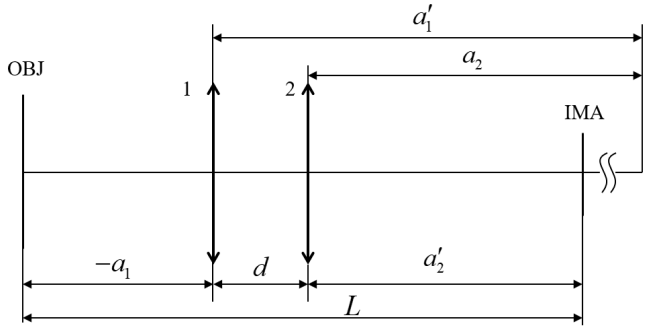

Figure 11 – Two-component relya lenses system consisting of two vario-lenses

Paraxial magnification of the image formed by lens 1,

$$\beta_1 = \frac{a_1'}{a_1}$$

From the Gauss formula [27] ,

$$a_1' = \frac{a_1 \cdot F_{1\text{var}}'}{a_1 + F_{1\text{var}}'} \quad \text{thus:}$$

$$\beta_1 = \frac{F_{1\text{var}}'}{a_1 + F_{1\text{var}}'}, \tag{24}$$

where $F_{1\text{var}}'$ is the back focal length of the vario-lens 1.

Transverse magnification of the secondary image formed by the vario-lens 2 ,

$$\beta_2 = \frac{a_2'}{a_2} \text{ , at a}$$

given fixed value of the segment and

$$a_2 = a_1' - d = \frac{a_1 \cdot F_{1\text{var}}'}{a_1 + F_{1\text{var}}'} - d\,, \tag{25}$$

is defined by the formula

$$\beta_2 = \frac{a_2'(a_1 + F_{1\text{var}}')}{(a_2' - L)F_{1\text{var}}' - a_1 d}. \tag{26}$$

In this case the required transverse magnification of the zoom-relay lenses is

$$\beta_1 \cdot \beta_2 = \beta\,, \tag{27}$$

Substituting (24) and (26) into formula (27) allows us to find the function:

$$F_{1\text{var}}'(\beta) = \frac{a_1 d \beta}{(a_1 - d)\beta - a_2'}. \tag{28}$$

The dependence $F_{1\text{var}}'(\beta)$ after its substitution into the formula (25) establishes the dependence $a_2(\beta)$. In this case, the back focal length of lens 2, providing the required value β , is determined by the expression:

$$F_{2\text{var}}'(\beta) = \frac{a_2(\beta) \cdot a_2'}{a_2(\beta) - a_2'}. \tag{29}$$

Formulas (28) and (29) allow not only to find dependences $F_{1\text{var}}'(\beta)$, $F_{2\text{var}}'(\beta)$, in the range of possible changes of optical forces of specific models of vario-lenses, but also to establish those specific values of a_1, d_1, a_2', L , at which it is possible to provide the required range of changes of value β .

Fig.12 shows as an example the graphs of optical powers of lenses 1 and 2 in dioptres: $D_{1\text{var}}(\beta) = \frac{1000}{F_{1\text{var}}'(\beta)}$, $D_{2\text{var}}(\beta) = \frac{1000}{F_{2\text{var}}'(\beta)}$, obtained at $a_1 = -80\,mm$, $d = 100\,mm$, $a_2' = 80\,mm$ using two identical Optotune ML-20-37 vario-lenses in the zoom-relay lenses, the working range of which $\pm 18\,dptr$ is marked on the plots by horizontal dotted lines.

The graphs show that the operating range of the first lens limits the range of linear magnification β to values $-0.5 \div -2.2$. If the range of lens 1 is shifted by an additional lens of fixed optical power by $+2\,dptr$, the range of values β , as can be seen from the graphs, expands to values $-0.5 \div -4$.

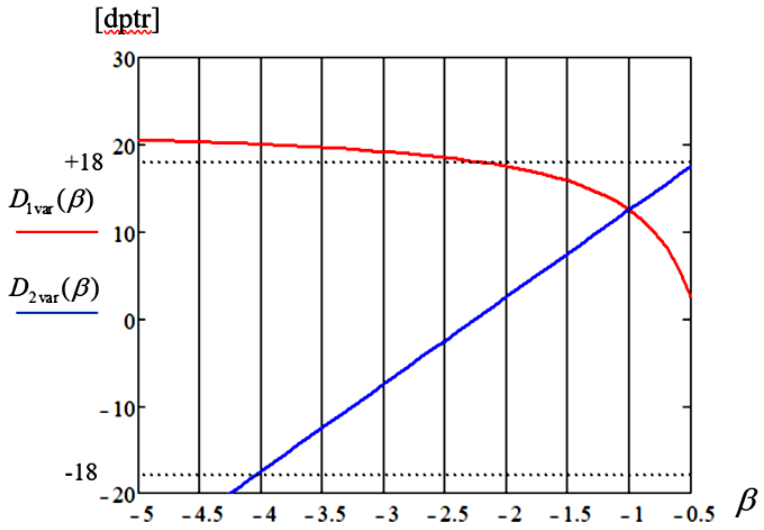

Figure 12 – Graphs of values of optical power of vario-lenses at change of paraxial magnification relay-lens system

The linear character of the function $D_{2\,var}(\beta)$ is easily realized by means of a stepper rotary motor, on the shaft of which there is a toothed wheel forming a kinematic pair with the outer toothed ring of the ML-20-37 lens.

2.3.1 Maximum field of zoom-relay lenses

In the zoom projection systems shown in Fig. 10, there is no intermediate real image, which does not allow to have a stationary field aperture in the system, unless it is the frame of the matrix photodetector mounted in the IMA plane, Figure11 In the zoom projection systems shown in Fig. 10, there is no intermediate real image, which does not allow to have a stationary field aperture in the system, unless it is the frame of the matrix photodetector mounted in the IMA plane, Figure11.

Therefore, in such systems one of the frames of variolenses serves as an aperture aperture diaphragm, the other - as a vignetting diaphragm, which limits the field of view of the system. But the roles of frames in such systems can change depending on the value of β In confirmation of this, Figure 13 shows the course of two axial fan of rays - axial and off-axis in the zoom-relay lens, which consists of two identical ML-20-37 vario-lenses at the values of intervals a_1, d, a_2', L , specified above.

As will be shown below in this zoom-relay lens, for a range of values β from -0.5 to -1, the aperture diaphragm is the frame the second lens, Figures.13 (a), (b), the frame of the first lens acting as a vignette.

In the range of values β from -1 onwards, the aperture diaphragm is the frame of the first lens, Figures 13 (c), (d), the frame of the second lens is the vignette diaphragm.

In Figsures 13 (a) and (c), the peripheral fan of rays is not vignetted. This means that its vignetting factors is $k = 1$.

In Figures 13 (b), (d), the peripheral fan of rays is fully vignetted, which means that the vignetting factors for fans ray is $k = 0$.

We will define the field of view of the system in the OBJ plane for values $k = 1$, within which there is no vignetting. And also for value $k = 0$, when outside such a field the image is completely absent due to complete non-passage of rays.

The aperture diaphragm of the system (STO) is not difficult to detect by determining the height of the beam on the second lens, provided the beam leaves the axial point of the plane OBJ and passes through the edge of the frame of the first vario-lens, Figure 14.

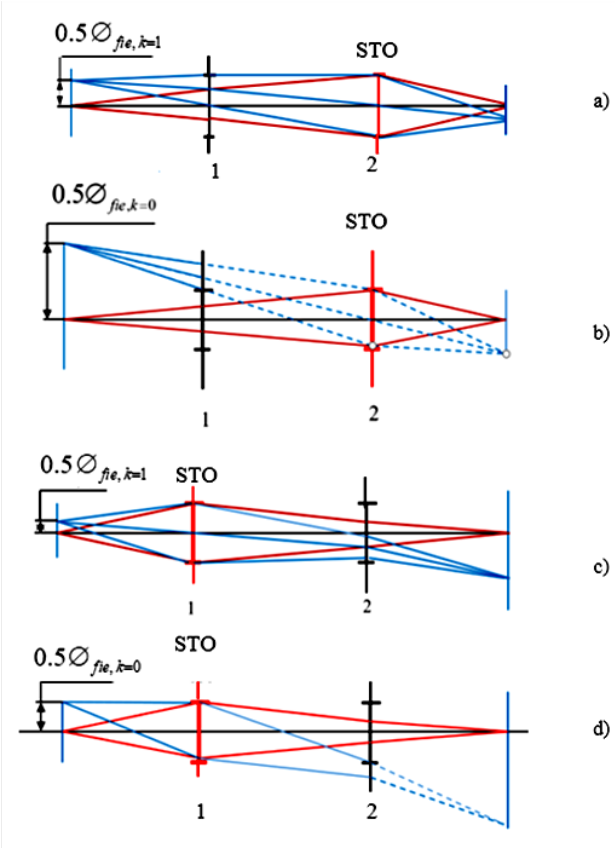

Figure 13. Course of the axial beam of rays (red) ; / off-axis beam of rays (blue):
a) , c) off-axis beam without vigniting;
b) , d) off-axis beam fully vigniting.

At the exit from the first lens the ray, depending on the value of its focal length, can follow the trajectory 1, Figure 14, then the frame of the first lens limits the axial fan of rays and it is aperture (STO), and the frame of the second lens serves as a vignetting.

In the case when the ray will follow the trajectory 2, Figure 14, the axial fan of rays is limited by the second aperture and it acts as an aperture diaphragm, while the frame of the first lens is a vignetting.

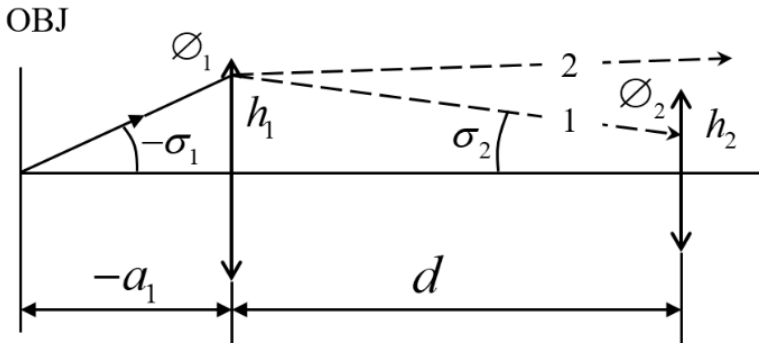

Figure 14 – Toward the identification of STO of the diaphragm

Applying this method to identify the roles of apertures at different values of β gives the following result:

If
$$F'_{1\text{var}}(\beta) > \frac{a_1 d}{a_1\left(1-\frac{\varnothing_2}{\varnothing_1}\right)-d} \tag{30}$$

where $F'_{1\text{var}}(\beta)$ is the focal length of the first lens, $\varnothing_1$, $\varnothing_2$ are the diameters of the apertures of the frames of the first and second lens, respectively, then the aperture diaphragm (DSTO) is the frame of the second lens, and the frame of the first lens is the vignette diaphragm.

In the case when $F'_{1\text{var}}(\beta)$ is less than the right part of formula (30), the role of the aperture diaphragm (STO) is transferred to the frame of the first lens, and the frame second lens becomes a vignetting diaphragm. The problem is considerably simplified when $\varnothing_2 = \varnothing_1$. Then $F'_{1\text{var}}(\beta)$ need only be compared with the segment $-a_1$.

If the aperture diaphragm serves as an aperture frame lens 1, the diameter of the maximum field of view at $k = 1$:

$$\varnothing_{fie,k=1} = \frac{a_1}{d}\left[(\varnothing_1 - \varnothing_2) - \varnothing_1 d\left(\frac{1}{a_1} + \frac{1}{F'_{1\text{var}}(\beta)}\right)\right]. \tag{31}$$

If the aperture diaphragm (STO) is the frame of lens 2, the diameter of the maximum field of view at :

$$\varnothing_{fie,k=1} = \frac{a_1}{d}\left[(\varnothing_2 - \varnothing_1) + \varnothing_1 d\left(\frac{1}{a_1} + \frac{1}{F'_{1\text{var}}(\beta)}\right)\right]. \tag{32}$$

In both cases, when the aperture diaphragm is the frame of the first or second lens, the diameter of the maximum field at is determined by the formula

$$\varnothing_{fie,k=0} = \frac{a_1}{d}\left[\varnothing_1 d\left(\frac{1}{a_1} + \frac{1}{F'_{1\text{var}}(\beta)}\right) - (\varnothing_1 + \varnothing_2)\right]. \tag{33}$$

Fig. 15 shows graphs of the diameter of the field of view of the zoom relay lens , calculated by formulas (31) - (33) for the system with vario-lenses ML-20-37 at values of intervals $a_1 = -80\,\text{mm}$, $d = 100\,\text{mm}$, $a'_2 = 80\,\text{mm}$.

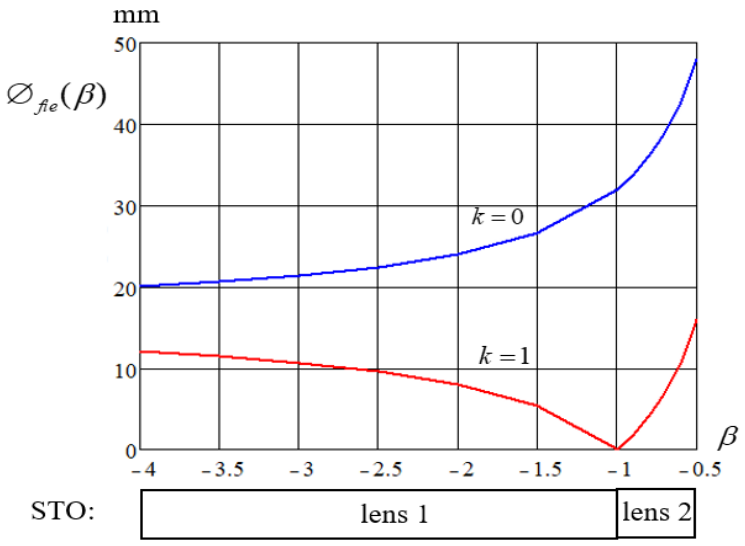

Figure 15 – Graphs of maximum field sizes in the absence of vignetting and at full vignetting of the outermost ray beam

The graphs show that as the absolute value of β decreases, the diameter of the field of view in the OBJ plane in the absence of vignetting ($k=1$) decreases to zero at $\beta=-1$ and then increases. The diameter of the maximum field, limited by full vignetting of the ray beams

($k=0$), increases monotonically, at that it considerably exceeds the field diameter at ($k=1$).

3. CONCLUSIONS

The material presented here shows that the main types of optical systems - lenses with image autofocusing, zoom-afocal optical systems, zoom-relay optical systems can be created by two immobile vario-lenses. External paraxial parameters of the specified zoom systems, their dimensions are essentially limited by the range of optical powers of the applied vario-lenses, as well as by the diameters of their aperture diaphragms. The degree of these limitations is shown on examples of creation of the considered zoom-optical systems with application of one of the best vario-lenses of Optotune ML-20-37. The operating range of optical power of this lens and the diameter of its aperture diaphragm of 20 mm are currently close to the physically maximum possible. The results of the analysis of zoom-afocal and zoom-relay optical systems show that the expansion of the range of paraxial and angular magnifications requires both an increase in the axial dimension of these systems and an increase in the optical power of variolenses. It is shown that in case of need to have a value of optical power of variolens, which is beyond the working range, it is possible to shift the range of optical power in one or another direction by using an additional lens with a fixed value of optical power, installing it next to the variolens. The fact of the influence of the displacement along the optical axis of the interface between two liquid media in vario-lenses at variations of their optical power requires additional study. This displacement leads to an axial displacement of the principal planes of the variolens and a possible small change in the parameters of the optical system, which needs to be taken into account when forming the control actions of the drivers of these lenses.

REFERENCES

1. Introduction to adaptive lenses / Shin-Tson Wu, Hongwen Ren ISBN 978-1-118-01899-6 References and links 1. M. Ye and S. Sato, “Optical properties of liquid crystal lens of any size,” Jpn. J. Appl. Phys. 41, L571-L573 (2002).
2. B. Wang, M. Ye, M. Honma, T. Nose, and S. Sato, “Liquid crystal lens with spherical electrode,” J pn. J. Appl. Phys. 41, L1232-L1233 (2002).
3. H. Ren Y. H. Fan, S. Gauza, and S. T. Wu, “Tunable-focus flat liquid crystal spherical lens,” Appl. Phys. Lett. 84, 4789- 4791 (2004).
4. X. Wang, H. Dai, and K Xu, “Tunable reflective lens array based on liquid crystal on silicon,” Opt. Express 13, 352-357 (2005).
5. N. Chronis, G. L. Liu, K. H. Jeong, and L. P. Lee, “Tunable liquid-filled microlens array integrated with microfluidic network,” Opt. Express 11, 2370-2378 (2003).
6. K. S. Hong, J. Wang, A. Sharonov, D. Chandra, J. Aizenberg, and S. Yang, “Tunable microfluidic optical devices with an integrated microlens array,” J. Micromech. Microeng. 16, 1660-1666 (2006).
7. J. Chen, W. Wang, J. Fang, and K. Varahramtan, “Variable-focusing microlens with microfluidic chip,” J. Micromech. Microeng. 14, 675-680 (2004).
8. H. Ren and S. T. Wu, “Variable-focus liquid lens,” Opt. Express 15, 5931-5936 (2007).
9. T. Krupenkin, S. Yang, and P. Mach, “Tunable liquid microlens,” Appl. Phys. Lett. 82, 316-318 (2003).
10. S. Kuiper and B. H. W. Hendriks, “Variable-focus liquid lens for miniature cameras,” Appl. Phys. Lett. 85, 1128-1130 (2004). terephthalate) insulating films,” Polymer 37, 2465-2470 (1996).
11. C. C. Cheng and J. A. Yeh, “Dielectrically actuated liquid lens,” Opt. Express 15, 7140-7145 (2007).
12. H. Ren and S. T. Wu, “Tunable-focus liquid microlens array using dielectrophoretic effect,” Opt. Express 16, 2646- 2652 (2008).
13. H. Ren, D. Fox, B. Wu, and S. T. Wu, “Liquid crystal lens with large focal length tunability and low operating voltage,” Opt. Express 15, 11328 (2007).

14. S. Gauza, H. Wang, C. H. Wen, S. T. Wu, A. J. Seed, and R. Dabrowski, “High birefringence isothiocyanato tolane liquid crystals,” Jpn. J. Appl. Phys. Part 1, 42, 3463-3466 (2003).
15. S. Gauza, C. H. Wen, S. T. Wu, N. Janarthanan, and C. S. Hsu, “Super high birefringence isothiocyanato biphenyl-bistolane liquid crystals,” Jpn. J. Appl. Phys. 43, 7634-7638 (2004).
16. J. D. Jackson, Classical Electrodynamics (Viley, New York, 1975), 2nd ed.
17. T. Krupenkin, S. Yang, and P. Mach, “Tubable liquid microlens,” Appl. Phys. Lett. 82, 316–318 (2003). G. C. Knollman, J. L. Bellin, and J. L. Weaver, “Variable-focus liquid-filled hydroacoustic lens,” J. Acoust. Soc. Am. 49, 253–261 (1971).
18. N. Sugiura and S. Morita, “Variable-focus liquid-filled optics lens,” Appl. Opt. 32, 4181–4186 (1993). [PubMed]
19. D. Y. Zhang, V. Lien, Y. Berdichevsky, J. Choi, and Y. H. Lo, “Fluidic adaptive lens with high focal length tenability,” Appl. Phys. Lett. 82, 3171–3172 (2003).
20. K. H. Jeong, G. L. Liu, N. Chronis, and L. P. Lee, “Tunable microdoublet lens array,” Opt. Express 12, 2494–2500 (2004). [PubMed]
21. P. M. Moran, S. Dharmatilleke, A. H. Khaw, and K. W. Tan, “Fluid lenses with variable focal length,” Appl. Phys. Lett. 88, 041120 (2006).
22. H. Ren, D. Fox, P. Anderson, B. Wu, and S. T. Wu, “Tunable-focus liquid lens controlled using a servo motor,” Opt. Express 14, 8031–8036 (2006). . [PubMed]
23. H. Ren, Y. H. Fan, S. Gauza, and S. T. Wu, “Tunable flat liquid crystal spherical lens,” Appl. Phys Lett. 84, 4789–4791 (2004).
24. E. Hecht, Optics, 4th edition (Addison Wesley, New York, 2002).
25. https://www.corning.com/worldwide/en/products/advanced-optics/product-materials/corning-varioptic-lenses.html
26. https://www.optotune.com/downloads
27. Chyzh, I. G. Theory of optical systems. Textbook [Electronic resource] : Electronic text data. – Kyiv: Igor Sikorsky Kyiv Polytechnic Institute, 2021. - 426 c. https://ela.kpi.ua/handle/123456789/46029.2
28. Pavlov, S.V., Kozhukhar, A. T., Electro-optical system for the automated selection of dental implants according to their colour matching, Przegląd elektrotechniczny, ISSN 0033-2097, R. 93 NR 3, 2017, pp. 121-124.
29. Kholin. V. V., Chepurna, O. M., Pavlov S., Methods and fiber optics spectrometry system for control of photosensitizer in tissue during photodynamic therapy, Proc. SPIE 10031, Photonics Applications in Astronomy, Communications, Industry, and High-Energy Physics Experiments 2016, 1003138.
30. Rovira, R. H., Tuzhanskyy, S., Pavlov, S. V., Savenkov, S. N., Kolomiets I. S., Polarimetric characterisation of histological section of skin with pathological changes, Proc. SPIE 10031, Photonics Applications in Astronomy, Communications, Industry, and High-Energy Physics Experiments 2016, 100313E.
31. Zabolotna, N. I.; Pavlov S. V., Radchenko, K. O.; Stasenko, V. A. , Wójcik, W., Diagnostic efficiency of Mueller-matrix polarization reconstruction system of the phase structure of liver tissue, Proc. SPIE 9816, Optical Fibers and Their Applications, 2015, 98161E.
32. Pavlov S. V. Information Technology in Medical Diagnostics //Waldemar Wójcik, Andrzej Smolarz, July 11, 2017 by CRC Press - 210 Pages.
33. Wójcik W., Pavlov S., Kalimoldayev M. Information Technology in Medical Diagnostics II. London: (2019). Taylor & Francis Group, CRC Press, Balkema book. – 336 Pages.

Надійшла до редакції 10.05.2025р.

CHYZH IGOR - D.Sc., professor, Department of Computer-Integrated Optical and Navigation Systems, Instrument Making Faculty, National Technical University of Ukraine “Igor Sikorsky Kyiv Polytechnic Institute, 03056 Kyiv, Ukraine; ***e-mail: deanpb@kpi.ua,*** ORCID: https://orcid.org/0000-0002-9565-1951

TYMCHYK GRYGORIJ - D.Sc., professor , Department of Devices Production, Instrument Making Faculty, National Technical University of Ukraine "Igor Sikorsky Kyiv Polytechnic Institute, 03056 Kyiv, Ukraine; ***e-mail: deanpb@kpi.ua,*** ORCID: https://orcid.org/0000-0003-1079-998X

GUBIYCHUK ROMAN - Master's student of the Faculty of Instrument Engineering, National Technical University of Ukraine "Igor Sikorsky Kyiv Polytechnic Institute, 03056 Kyiv, Ukraine; ***e-mail: gubiychuk@gmail.com***

KARAS OLEKSANDR— Doctor of Philosophy, Senior Lecturer, Department of Biomedical Engineering and Optoelectronic Systems, Vinnytsia National Technical University, Vinnytsia, ***e-mail: karas@vntu.edu.ua***

ІГОР ЧИЖ, ГРИГОРІЙ ТИМЧИК, РОМАН ГУБІЙЧУК, ОЛЕКСАНДР КАРАСЬ

ZOOM VARIO-OPTICAL SYSTEMS OF OPTOELECTRONIC SENSORS WITH IMMOBILE COMPONENTS

Національний технічний університет України «Київський політехнічний інститут імені Ігоря Сікорського», 03056 Київ, Україна
Вінницький національний технічний університет, Україна